THE AMERICAN SOCIETY OF MECHANICAL ENGINEERS
345 E. 47 St., New York, N.Y. 10017

86-GT-242

Multiaxial Life Prediction System for Turbine Components

S. T. ARVANITIS
Senior analytical engineer
Y. B. SYMKO
Senior analytical engineer
R. N. TADROS
Chief structures & dynamics
Pratt and Whitney Canada Inc.
Montreal, Canada

ABSTRACT

The objective of this paper is to present a complete 3-D life prediction system which was developed for turbine engine components. It will primarily deal with turbine blades and vanes which are subjected to hostile thermal and combustion environments under load which creates cyclic and/or steady multiaxial stress and strain fields. All of the above factors combined are detrimental to the service life of these components and need very careful consideration at the design stage.

The developed multiaxial system for a mission includes evaluation of transient metal temperatures, corresponding elastic and inelastic strains, creep strains and subsequently creep/fatigue lives. The calculations are performed using the ductility exhaustion method. The maximum principal normal strain ranges used in the life analysis are found by a developed procedure for a multi-axial system. The concept is based on analyzing all of the time steps computed in the mission, in order to develop the maximum principal normal strain range whose direction and magnitude is strictly a function of the component geometry and mission loading. The mission creep is then developed by maximizing a cumulative creep function. Directional consistency is maintained in accumulating creep/fatigue damage with respect to the incurred multiaxial stress and strain fields. Also the most damaging mission modes(creep or fatigue) will be separated. Further development in the model includes the capability of analytically obtaining the fatigue curve for any ratio (R) of minimum to maximum strain using baseline fatigue material properties (R=-1.0). Application of the model to an actual uncooled vane correlates well with test rig development experience.

NOMENCLATURE

A,B,C,D	Creep function constant
$A,B_{mission}$	Mission creep constants
a,b	Fatigue ductility exponent and coefficient
F_p, F_s, F_t	Primary, secondary & tertiary creep curves
k	Operational index
K	Subscript refers to creep mission condition
m	Number of mission calculation points
No, N	Number of fatigue cycles to failure
N'	Number of cycles after an elapsed 1/4 cycle
N_P	Number of cycles repeated at a strain range
N.C.C.	Number of creep conditions in mission
R	Strain ratio on maximum absolute strain
t	Time
t_K	Hold time at mission condition
t_{E_1} ,t_{E_2}	Incremental creep times elapsed in mission
t_{EQ_1},t_{EQ_2}	Equivalent creep time to fatigue cycles
x, y, z	Cartesian coordinate system
ε_{ij}	Strain tensor
$\Delta\varepsilon_{ij}$	Strain difference between time instances
ε_f	Fracture strain in monotonic tension
ε_{max}	Maximum strain
ε_m	Mean strain
ε_{min}	Minimum strain
ε_n	Normal strain
ε_o	Initial strain upon loading
ε_{cum}	Cumulative creep function for mission
λ	Lagrange multiplier or eigenvalue
θ_x, θ_y, θ_z	Orientation angles for normal strain tensor
θ_{xp}, θ_{yp}, θ_{zp}	Principal angles for normal strain range
σ_{ij}	Stress tensor
Superscript	
c	relating to creep

INTRODUCTION

Modern gas turbine engines are required to produce a large amount of thrust or shaft horsepower and also withstand very severe thermal conditions and high loads which arise during cyclic mission operation. The engine hot section experiences the full effect of the above factors because it is this section of the engine which develops power. Subsequently most of the life problems are encountered in this area. Typical failure modes are listed for each of the components that suffer degradation during engine operation, ie., combustor liners(thermal fatigue, creep buckling and corrosion), seals(wear), disks(low cycle fatigue), vanes(thermal low cycle fatigue and corrosion), and blades(thermal and high and low cycle fatigue, creep and corrosion).

In order to determine the life of these components at the design stage one begins with a determination of

Presented at the International Gas Turbine Conference and Exhibit
Dusseldorf, West Germany—June 8-12, 1986

the operating environment and a calculation of the thermal and mechanical loading to which they are subjected. With the exception of the centrifugal loads on the blades and disks, the primary source of fatigue loading is due to the severe thermal cycling associated with each start-up and shut-down of the engine, although high-frequency excitation problems are sometimes encountered as well.

Low-cycle fatigue and thermal fatigue occur in component parts at highly localized regions. The strain in such small localized regions is larger than the surrounding region as a result of notches that concentrate it, or of constrained thermal expansion as in the case of thermal fatigue. The key feature is that the local strain is prevented from exceeding certain bounds due to the surrounding material which remains elastic. Hence, the local material is caused to cycle between approximately constant strain limits. When the local strains are large, inelastic strain occurs and the cyclic stress-strain behavior becomes non-linear.

Creep damage is primarily encountered by turbine blades and combustion chambers which are subjected to constant centrifugal loading and internal gas pressure respectively, in conjunction with high thermal gradients. Under creep, blades deform up to the point where interference occurs with the shroud or rupture thus limiting their useful life.

During the course of a mission these components are subjected to a combination of creep and fatigue which gives rise to cyclic damage accumulation and subsequently failure. To accurately determine these cyclic lives it becomes necessary to compute the transient and steady state temperatures and the elastoplastic and creep strains of the component, using the engine mission. Past practice in airfoil inelastic stress analysis has been to use programs based on the beam theory assumption that plane sections remain plane. However this practice produces very pessimistic airfoil lives due to the conservative nature of beam theory. In recent years non-linear finite element computer programs have been developed that perform three dimensional thermal, elasto-plastic stress and creep analysis. These non-linear computer programs have been primarily used at engine development stages due to the extensive work and computing times involved. Once the cyclic stress-strain and creep behavior of the engine materials has been determined a finite element structural analysis may be performed. The results of the analyses are the local three dimensional stress-strain-temperature versus time response of the material at the most critical locations in the component part. Finally, from a knowledge of the fatigue, creep and fracture resistance of the materials, a prediction of the lifetime of the component part can be made.

This paper will focus primarily on the progress of the development of a multiaxial life prediction system using the ductility exhaustion approach. Application to a typical uncooled vane will also be described.

MULTIAXIAL CREEP/FATIGUE MODEL

The components employed in the engine hot section are subjected to extremely high temperatures and corrosive environments in conjunction with high external loads. These components must retain adequate strength at high temperatures. In order to achieve this, cast nickel based superalloys are used. The characteristics of these superalloys are good high temperature creep strength and low ductility along with good high temperature corrosion resistance. As a consequence these materials exhibit brittleness.

Tensile test results indicate that both shearing and normal stresses under axial loading are important in distinguishing the type of fracture. A brittle material loaded in tension will fail on the transverse plane, whereas a ductile material loaded in tension will fail in shear on the 45 degree plane. Therefore the concept of maximum principal normal stress or strain becomes very important in any life evaluation concerning brittle materials.

Mission Maximum Principal Normal Strain Range and corresponding Mean Strain

In a turbine component mission, there will generally exist various strain cycles or subcycles along with constant condition time periods. A typical component will experience a triaxial stress or strain field. Due to the uniaxial nature of strain controlled fatigue tests all data refers to a principal normal strain range value.

It now becomes important to develop a set of relations enabling one to evaluate the maximum principal normal strain range for a triaxial strain field varying in time. Figure 1 depicts a general triaxial state of strain also showing the normal strain tensor acting in an arbitrary direction defined by three angles ($\theta_x, \theta_y, \theta_z$).

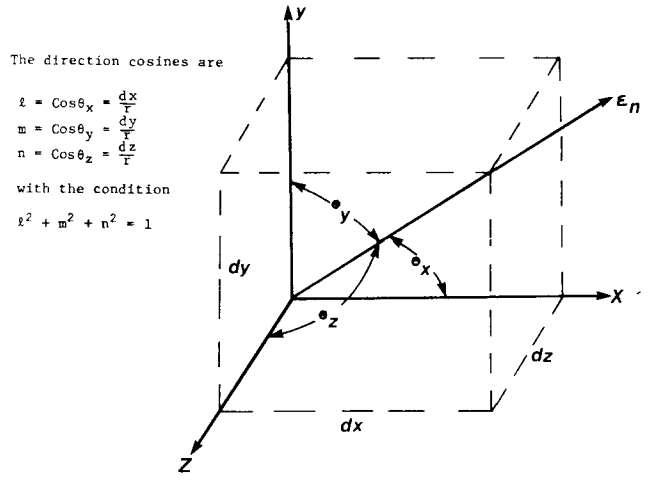

FIG. 1 TRIAXIAL STATE OF STRAIN SHOWING NORMAL STRAIN TENSOR

The normal strain (Reference 1) may be written as a function of θ_x, θ_y, θ_z and all of the strain components ε_x, ε_y, ε_z, ε_{xy}, ε_{xz}, ε_{yz} as follows

$$\varepsilon_n = \varepsilon_x \ell^2 + \varepsilon_y m^2 + \varepsilon_z n^2 + 2\varepsilon_{xy}\ell m + 2\varepsilon_{xz}\ell n + 2\varepsilon_{yz} mn \qquad (1)$$

In a typical mission cycle or subcycle there will be " k = 1, m" strain points as shown in figure 2.

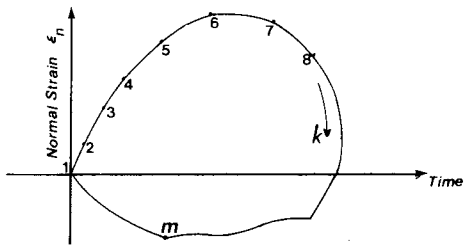

FIG. 2 TYPICAL MISSION CYCLE WITH k = 1, m STRAIN POINTS

In order to obtain the maximum principal normal strain range over the mission cycle or subcycle it will become

necessary to evaluate

$$\sum_{k=1}^{m} (k - 1) \qquad (2)$$

principal normal strain ranges. The normal strain range at any point in a component between any two mission times "k" and " k-1 " is defined as follows:

$$\Delta\varepsilon_n(\theta_x,\theta_y,\theta_z) = |\varepsilon_n(\theta_x,\theta_y,\theta_z)_{k-1} - \varepsilon_n(\theta_x,\theta_y,\theta_z)_k| \qquad (3)$$

In order to be consistent with the definition of strain range and also with uniaxial strain controlled fatigue data, the directions of the normal strains at the two time instances " k " and " k-1 " must be the same. Thus the expression for the strain range derived from equation (3) now takes on the following form:

$$\Delta\varepsilon_n = |\Delta\varepsilon_x \ell^2 + \Delta\varepsilon_y m^2 + \Delta\varepsilon_z n^2 + 2\Delta\varepsilon_{xy}\ell m + 2\Delta\varepsilon_{xz}\ell n + 2\Delta\varepsilon_{yz} mn| \qquad (4)$$

where the strain difference components are

$$\begin{aligned} \Delta\varepsilon_x &= \varepsilon_{x_k} - \varepsilon_{x_{k-1}} & \Delta\varepsilon_{xy} &= \varepsilon_{xy_k} - \varepsilon_{xy_{k-1}} \\ \Delta\varepsilon_y &= \varepsilon_{y_k} - \varepsilon_{y_{k-1}} & \Delta\varepsilon_{xz} &= \varepsilon_{xz_k} - \varepsilon_{xz_{k-1}} \\ \Delta\varepsilon_z &= \varepsilon_{z_k} - \varepsilon_{z_{k-1}} & \Delta\varepsilon_{yz} &= \varepsilon_{yz_k} - \varepsilon_{yz_{k-1}} \end{aligned} \qquad (5)$$

The principal normal strain range will occur parallel to a plane oriented at three principal angles θ_x, θ_y, θ_z. In order to determine the three principal angles and thus the principal normal strain range, equation (4) must be maximized with respect to θ_x, θ_y, θ_z which are constrained by the following

$$\ell^2 + m^2 + n^2 = 1 \qquad (6)$$

When a condition such as (6) is imposed on a function such as (4), the problem of determining the maximum and minimum of that function is called a problem of constrained maxima and minima with a side condition. By employing Lagrange multipliers the above problem may be transformed to a free maxima and minima problem. The expression for the strain range becomes as follows

$$\Delta\varepsilon_n(\theta_x,\theta_y,\theta_z,\lambda) = \Delta\varepsilon_n(\theta_x,\theta_y,\theta_z) + \lambda(\ell^2 + m^2 + n^2 - 1) \qquad (7)$$

The condition for stationary value is applied

$$\begin{aligned} \frac{\partial}{\partial\theta_x}\Delta\varepsilon_n(\theta_x,\theta_y,\theta_z,\lambda) &= 0 \\ \frac{\partial}{\partial\theta_y}\Delta\varepsilon_n(\theta_x,\theta_y,\theta_z,\lambda) &= 0 \\ \frac{\partial}{\partial\theta_z}\Delta\varepsilon_n(\theta_x,\theta_y,\theta_z,\lambda) &= 0 \end{aligned} \qquad (8)$$

to yield a set of equations in matrix form

$$\begin{bmatrix} \Delta\varepsilon_x + \lambda & \Delta\varepsilon_{xy} & \Delta\varepsilon_{xz} \\ \Delta\varepsilon_{yx} & \Delta\varepsilon_y + \lambda & \Delta\varepsilon_{yz} \\ \Delta\varepsilon_{zx} & \Delta\varepsilon_{zy} & \Delta\varepsilon_z + \lambda \end{bmatrix} \begin{Bmatrix} \mathrm{Cos}\,\theta_x \\ \mathrm{Cos}\,\theta_y \\ \mathrm{Cos}\,\theta_z \end{Bmatrix} = \begin{Bmatrix} 0 \\ 0 \\ 0 \end{Bmatrix} \qquad (9)$$

This is now a standard eigenproblem, where λ refers to the eigenvalue and $\mathrm{Cos}\,\theta_x$, $\mathrm{Cos}\,\theta_y$, $\mathrm{Cos}\,\theta_z$ to the eigenvector . The solution of (9) will yield three eigenvalues (or principal Strain ranges) and each eigenvalue will subsequently give rise to a eigenvector (or principal directions). The largest eigenvalue gives the principal value of maximum normal strain range and its three principal directions are obtained from the corresponding eigenvector, ie

$$\Delta\varepsilon_n,\ \theta_{xp},\ \theta_{yp},\ \theta_{zp} \qquad (10)$$

The above procedure is followed for all combinations in the mission cycle or subcycle (equation 2) until the maximum principal normal mission (cycle or subcycle) strain range is determined. The corresponding principal angles θ_{xp}, θ_{yp}, θ_{zp} may now be employed to determine the mean strain and ratio (R) of minimum to maximum or maximum to minimum strain as follows. By definition the mean strain acting in the direction of the maximum principal normal strain range is

$$\varepsilon_m(\theta_{xp},\theta_{yp},\theta_{zp}) = \tfrac{1}{2}|\varepsilon_n(\theta_{xp},\theta_{yp},\theta_{zp})_k + \varepsilon_n(\theta_{xp},\theta_{yp},\theta_{zp})_{k-1}| \qquad (11)$$

The ratio R is defined as follows:

$$\text{for } |\varepsilon_n(\theta_{xp},\theta_{yp},\theta_{zp})_{k-1}| > |\varepsilon_n(\theta_{xp},\theta_{yp},\theta_{zp})_k|, \quad R = \frac{\varepsilon_n(\theta_{xp},\theta_{yp},\theta_{zp})_k}{\varepsilon_n(\theta_{xp},\theta_{yp},\theta_{zp})_{k-1}}$$

$$\text{for } |\varepsilon_n(\theta_{xp},\theta_{yp},\theta_{zp})_k| < |\varepsilon_n(\theta_{xp},\theta_{yp},\theta_{zp})_{k-1}|, \quad R = \frac{\varepsilon_n(\theta_{xp},\theta_{yp},\theta_{zp})_{k-1}}{\varepsilon_n(\theta_{xp},\theta_{yp},\theta_{zp})_k} \qquad (12)$$

Evaluation of Principal Normal Mission Creep

During the course of an operating mission, hot turbine components are subjected to long constant loading time periods which causes them to slowly permanently deform. At high temperatures this slow plastic deformation or creep deformation, may proceed indefinitely and eventually the material fractures. The creep curve exhibits various stages. Directly on loading, the component undergoes an instantaneous strain. This is followed by the primary stage. The creep rate declines gradually in this region and eventually reaches a constant (steady state) value in the secondary stage. In the tertiary stage the creep rate starts to accelerate and this leads to final fracture. Usually material creep data are obtained from uniaxial tests at various conditions. It is generally a function of the following variables, ie

$$\varepsilon^c_{ij} = F(\sigma_{ij},t,T) \qquad (13)$$

Where the σ_{ij} are the creep stresses, ε^c_{ij} are the creep strain components, and t and T are respectively time and temperature. The three stages of creep (primary, secondary, tertiary) may be described by a suitable piecewise continuous function, ie

$$\varepsilon^c_{ij} = F_p(\sigma_{ij},t,T) + F_s(\sigma_{ij},t,T) + F_t(\sigma_{ij},t,T) \qquad (14)$$

Depending on the shape of the creep curve for the particular material in question the function described by equation (14) may be of polynomial or exponential form.

The treatment of the creep problem may be described best upon consideration of a typical engine mission shown in figure 3. As may be seen, this figure depicts an aircraft engine mission with four constant condition intervals, ground idle, take-off, cruise and ground idle.

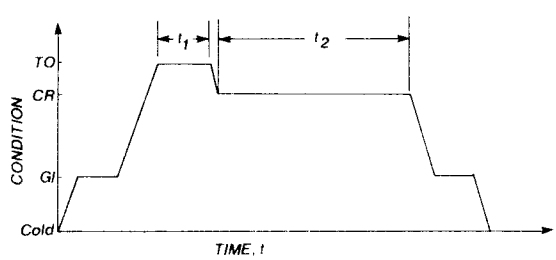

FIG. 3 TYPICAL AIRCRAFT ENGINE MISSION

As a simplified illustration of how the creep problem will be approached only the two most damaging creep conditions of take-off and cruise will be considered for analysis.

The component in question is analysed for creep under take-off and cruise conditions, separately (each condition is taken to rupture). The analytical tool to be employed is a 3-D F.E. creep analysis. Upon completion of the creep analysis for mission conditions 1 and 2 (fig. 3) the nodal distribution for creep strain in all directions will be obtained for both mission creep hold times as follows

$$\varepsilon^c_{ij}(t_1) \qquad \text{and} \qquad \varepsilon^c_{ij}(t_2) \tag{15}$$

Now having obtained all of the creep strain components as a function of time, for conditions 1 and 2 (Fig. 3) the expressions for the normal creep strain as a function of θ_x, θ_y, θ_z for each condition may now be developed as follows:

$$\varepsilon^c_n(t_1) = \varepsilon_x(t_1)\ell^2 + \varepsilon_y(t_1)m^2 + \varepsilon_z(t_1)n^2 + 2\varepsilon_{xy}(t_1)\ell m + 2\varepsilon_{xz}(t_1)\ell n + 2\varepsilon_{yz}(t_1)mn \tag{16}$$

and

$$\varepsilon^c_n(t_2) = \varepsilon_x(t_2)\ell^2 + \varepsilon_y(t_2)m^2 + \varepsilon_z(t_2)n^2 + 2\varepsilon_{xy}(t_2)\ell m + 2\varepsilon_{xz}(t_2)\ell n + 2\varepsilon_{yz}(t_2)mn \tag{17}$$

Where t_1 and t_2 are the mission cycle hold times at conditions 1 & 2 respectively.

The next step is to determine the direction of maximum accumulated creep damage. This may be found upon maximization of a cumulative creep function which is defined as follows:

$$\varepsilon^c_{cum}(\theta_x,\theta_y,\theta_z) = \sum_{K=1}^{NCC} \varepsilon^c_n(t_K,\theta_x,\theta_y,\theta_z) \tag{18}$$

Where N.C.C. represents the number of creep conditions under consideration in the mission. In order to determine the three principal normal creep directions equation (18) must be maximized with respect to θ_x, θ_y and θ_z. This is carried out with the constraint condition (equation 6) satisfied.

$$\varepsilon^c_{cum}(\theta_x,\theta_y,\theta_z,\lambda) = \sum_{K=1}^{NCC} \varepsilon^c_n(t_K,\theta_x,\theta_y,\theta_z) + \lambda(\ell^2+m^2+n^2-1) \tag{19}$$

Equation (19) may be solved by the Lagrange multiplier method by setting up the typical eigenvalue problem as was previously carried out for the principal normal strain range. In this case the eigenvalue with the maximum magnitude will be the principal normal cumulative creep strain and its corresponding eigenvector yields the principal directions, ie

$$\max\ \varepsilon^c_{cum},\ \theta^c_{xp},\ \theta^c_{yp},\ \theta^c_{zp} \tag{20}$$

Once the principal planes have been determined their values may be re-substituted into equations (16) and (17) to obtain functions of the form

$$\varepsilon^c_n(t_1,\theta^c_{xp},\theta^c_{yp},\theta^c_{zp}) \text{ and } \varepsilon^c_n(t_2,\theta^c_{xp},\theta^c_{yp},\theta^c_{zp}) \tag{21}$$

Upon consideration of conditions 1 and 2 and by using equations (21) and the life fraction rule it becomes an easy task to fit a general creep expression for the principal normal creep for the entire mission which in this case is assumed to be comprised of conditions 1 and 2 as follows:

$$\varepsilon_{mission}(t) = A_{mission}\, t^{B_{mission}} \tag{22}$$

Life Evaluation by Ductility Exhaustion

Use will now be made of the equations, derived in previous sections, concerning maximum principal value of normal strain range and principal normal mission creep. Creep and fatigue may now be combined, based on the ductility exhaustion model (Ref. 2), in order to evaluate component life.

Generally the fatigue behavior in the low cycle regime obeys the following relationship

$$N = b\ \Delta\varepsilon_n^{-a} \tag{23}$$

Where a is the fatigue ductility exponent defined by the slope of the $\Delta\varepsilon$ - N curve and b is the fatigue ductility coefficient given by the strain intercept. A typical total strain range versus fatigue curve is depicted in figure 4. From figure 4, ε_f is the

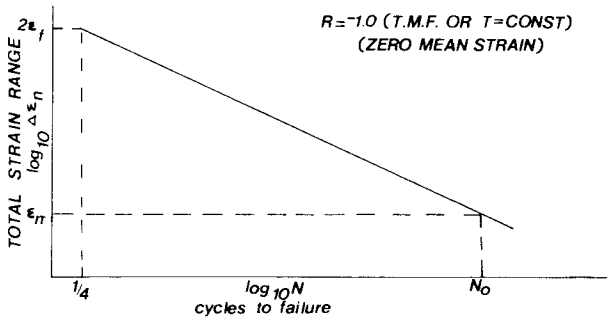

FIG.4 TYPICAL FATIGUE DIAGRAM

fracture strain in static tension and $N_{1/4}$ refers to one quarter of a cycle, thus:

$$No = b\ \Delta\varepsilon_n^{-a} \qquad \text{and} \qquad N_{1/4} = b\ \Delta\varepsilon_n^{-a} = \tfrac{1}{4} \tag{24}$$

Since

$$\frac{No}{N_{1/4}} = 4No = \left\{\frac{\Delta\varepsilon_n}{\Delta\varepsilon_{n_{1/4}}}\right\}^{-a}$$

thus

$$No = \tfrac{1}{4}\left\{\frac{2\varepsilon_f}{\Delta\varepsilon_n}\right\}^a$$

or, giving a relationship of the form

$$\Delta\varepsilon_n^a\ No = \text{constant} \tag{25}$$

The constant in the above equation (Ref. 2) may be considered as $(2\varepsilon_f)^a/4$ by interpreting a static tension test as 1/4 cycle with a strain range of twice the fracture strain ε_f. No is the number of cycles at which the material ductility has been exhausted for a strain range $\Delta\varepsilon_n$.

Knowing the above baseline stabilized hysterisis loop properties where R=-1.0 one may analytically generate or determine the life for any R-ratio by the approach adopted in Reference 3. Figure 5 shows a usual loading path for the first strain cycle with a

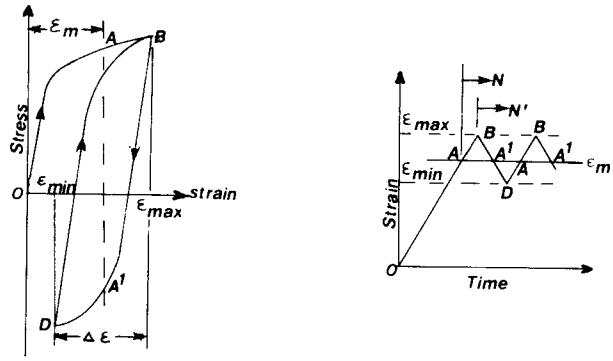

FIG.5 PROGRESSIVE STRAIN CYCLING ABOUT MEAN STRAIN

mean strain of ε_m. This diagram may be interpreted as follows. Strain is initially increased to its maximum value B and then is repeated between this maximum value B and the minimum value D. The number of cycles counted from the initial maximum point B is denoted by N'. The relationship between No and N' is given as

$$N' = No - \frac{1}{4} \tag{26}$$

In what follows, analytical equations expressed in terms of No will be derived. The damage due to initial straining to ε_{max} is given by $(2\ \varepsilon_{max})^a/4$. The number of cycles No to fracture is expressed as

$$\Delta\varepsilon_n^a\ (No - \tfrac{1}{4}) = \frac{(2\varepsilon_f)^a}{4} - \frac{(2\varepsilon_{max})^a}{4} \tag{27}$$

This equation can be rewritten as

$$\left[\frac{\Delta\varepsilon_n}{2\varepsilon_f}\right]^a (4No - 1) + \left[\frac{\varepsilon_{max}}{\varepsilon_f}\right]^a = 1 \tag{28}$$

A more convenient expression than the above is presented in terms of $\Delta\varepsilon_n$ and ε_m as follows

$$\left[\frac{\Delta\varepsilon_n}{2\varepsilon_f}\right]^a (4No - 1) + \left[\frac{\Delta\varepsilon_n}{2\varepsilon_f} + \frac{\varepsilon_m}{\varepsilon_f}\right]^a = 1 \tag{29}$$

In the case of compressive mean strain, ie., $|\varepsilon_{min}| > |\varepsilon_{max}|$, ε_{max} and ε_m in these equations should be replaced by $|\varepsilon_{min}|$ and $|\varepsilon_m|$ respectively. In other words, ε_{max} is defined as the maximum absolute value of strain. A more convenient way of expressing the foregoing equations is to use a strain ratio R, as defined in Eq. 12, where

$$\begin{aligned} R &= \frac{\varepsilon_{min}}{\varepsilon_{max}} \qquad \text{for } |\varepsilon_{max}| > |\varepsilon_{min}| \\ R &= \frac{\varepsilon_{max}}{\varepsilon_{min}} \qquad \text{for } |\varepsilon_{max}| < |\varepsilon_{min}| \end{aligned} \tag{30}$$

With R defined, the above equation, for $\Delta\varepsilon_n$, now becomes

$$\Delta\varepsilon_n = \frac{2(1-R)\ \varepsilon_f}{[(4No-1)(1-R)^a + 2^a]^{1/a}} \tag{31}$$

or,

$$No = \frac{1}{4}\left[1 + \left[\frac{2\varepsilon_f}{\Delta\varepsilon_n}\right]^a - \left[\frac{2}{1-R}\right]^a\right] \tag{32}$$

If the material were to be cycled to N_P cycles at a strain range $\Delta\varepsilon_n$ and if the original ductility were ε_f then the remaining ductility would be

$$\varepsilon_{f_i} = \varepsilon_f \left\{1 - \frac{N_P}{No}\right\}^{1/a} \tag{33}$$

This would imply the material has undergone a loss of ductility of

$$d\varepsilon = \varepsilon_f \left\{1 - \left[1 - \frac{N_P}{No}\right]^{1/a}\right\} \tag{34}$$

or,

$$d\varepsilon = \varepsilon_f \left[1 - \left[1 - \frac{4N_P}{1 + \left[\frac{2\varepsilon_f}{\Delta\varepsilon_n}\right]^a - \left[\frac{2}{1-R}\right]^a}\right]^{1/a}\right] \tag{35}$$

where $\Delta\varepsilon_n$ and R have been developed in Eq's 10 and 12.

The cumulative creep damage can be incorporated in this model by the method which will be described below. A typical creep curve for a given load and temperature is shown in Figure 6. Where

$$\varepsilon^c(t) = \varepsilon_o + At^B + Ct^D \qquad (B < 1 \text{ and } D > 1) \tag{36}$$

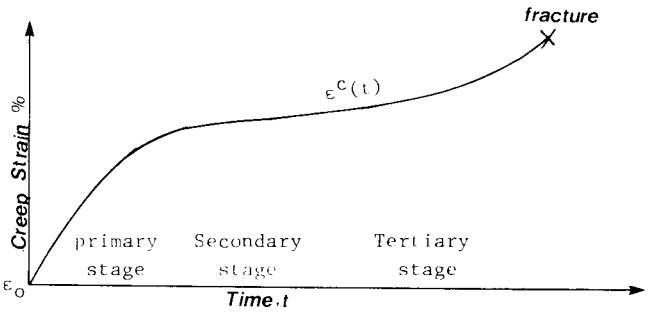

FIG. 6 TYPICAL CREEP CURVE

In general ε_o is taken as a reference point and the Ct^D term may dropped which reduces the above equation to

$$\varepsilon_n^c = At^B$$

or as previously derived (equation 22) for the entire creep mission of the component.

Since both cycling and creep are assumed to contribute to the same failure mechanism, the damage that resulted during the first increment in cycles is equivalent to an increment of creep strain, whose equivalent time is evaluated by knowledge of the mission creep parameters and the proper strain range. Thus

$$t_{EQ_1} = \left[\frac{d\varepsilon_1}{A_{mission}}\right]^{1/B_{mission}} \tag{37}$$

where

$$d\varepsilon_1 = \varepsilon_f\left[1 - \left[1 - \frac{4N_1}{1 + \left[\frac{2\varepsilon_f}{\Delta\varepsilon_{n_1}}\right]^a - \left[\frac{2}{1-R_1}\right]^a}\right]^{1/a}\right] \tag{38}$$

and is the ductility decrement which the material has undergone after N_1 cycles at a certain strain range $\Delta\varepsilon_{n_1}$ and ratio R_1. During the N_1 mission cycles or subcycles and elapsed mission time t_{E_1} some creep took place whose magnitude may be evaluated from the mission creep parameters as follows

$$\varepsilon_{mission} = A_{mission}\ t_{E_1}^{B_{mission}} \tag{39}$$

Now combining the creep and strain cycle the remaining system ductility will be

$$\varepsilon_{f_i} = \varepsilon_f - A_{mission}\ (t_{E_1} + t_{EQ_1})^{B_{mission}} \tag{40}$$

The solution proceeds with the addition of another increment of cycles or subcycles which may have the same strain amplitude or a different one. In either case, an additional decrement in ductility results, which is evaluated by replacing N_1, $\Delta\varepsilon_{n_1}$, ε_f and R_1 with N_2, $\Delta\varepsilon_{n_2}$, ε_{f_i} and R_2 respectively.

$$d\varepsilon_2 = \varepsilon_{f_i}\left[1 - \left[1 - \frac{4N_2}{1 + \left[\frac{2\varepsilon_{f_i}}{\Delta\varepsilon_{n_2}}\right]^a - \left[\frac{2}{1-R_2}\right]^a}\right]^{1/a}\right] \tag{41}$$

The equivalent creep time for the new decrement in ductility now becomes

$$t_{EQ_2} = \left[\frac{d\varepsilon_2}{A_{mission}}\right]^{1/B_{mission}} \tag{42}$$

Also during the second increment of subcycles there will exist an elapsed mission time t_{E_2} over which some

more creep took place and when it is combined with t_{EQ_2} it will give a remaining system ductility of

$$\varepsilon_{f_{i+1}} = \varepsilon_{f_i} - A_{mission} (t_E + t_{EQ})^{B_{mission}} \quad (43)$$

The above procedure is repeated until the remaining ductility is exhausted, and failure occurs. An evaluation of the life must be made by creep/fatigue interaction (or ductility exhaustion) by observing the following steps for each node of the finite element model.

(1)--Determine the maximum principal normal strain range (and θ_{xp}, θ_{yp}, θ_{zp}) and also the normal mean strain on this plane, for each mission cycle or subcycle.

(2)--Determine the mission principal normal creep parameters (and θ^c_{xp}, θ^c_{yp}, θ^c_{zp}).

(3)--Evaluate creep/fatigue life by exhausting the ductility in the maximum principal normal strain range direction (θ_{xp}, θ_{yp}, θ_{zp}) of each mission cycle or subcycle.

(4)--Evaluate creep/fatigue life by exhausting the ductility in the mission principal normal creep direction (θ^c_{xp}, θ^c_{yp}, θ^c_{zp}).

(5)--Select the lowest life (from 3 or 4) to determine the structural integrity of the turbine component.

UNCOOLED AIRFOIL STUDY

In order to evaluate the approach developed herein a typical integral uncooled low pressure turbine vane was analysed and the results of the analysis were then compared to a test rig study. The study was performed in four phases as follows: (i)finite element model generation (yielding 653 nodes and 75 twenty node isoparametric solid elements) (ii)finite element non-linear thermal mission analysis (iii)finite element elasto-plastic mission stress/strain analysis (iv)low cycle fatigue life analysis and comparison to test rig results.

Analytical Life Prediction

Due to the, primarily, constant strain nature of the mission experienced by the vane and also based on previous experience, it was assumed that the fatigue portion of the loading spectrum would be more detrimental to the life of this component rather than the creep portion.

The components' geometry and three-dimensional finite element model used for thermal, stress and life analyses are depicted in figures 7 and 8 respectively.

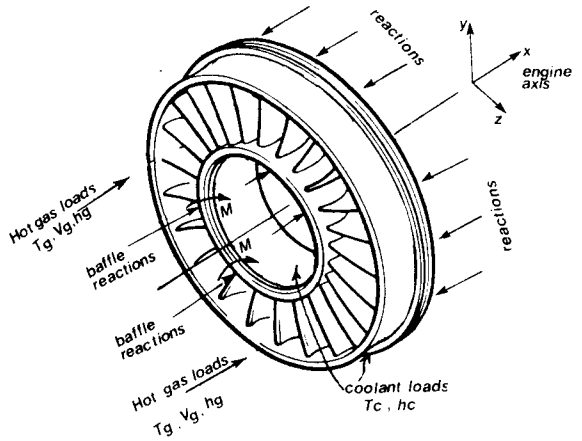

FIG.7 VANE RING AND LOADS ACTING UPON

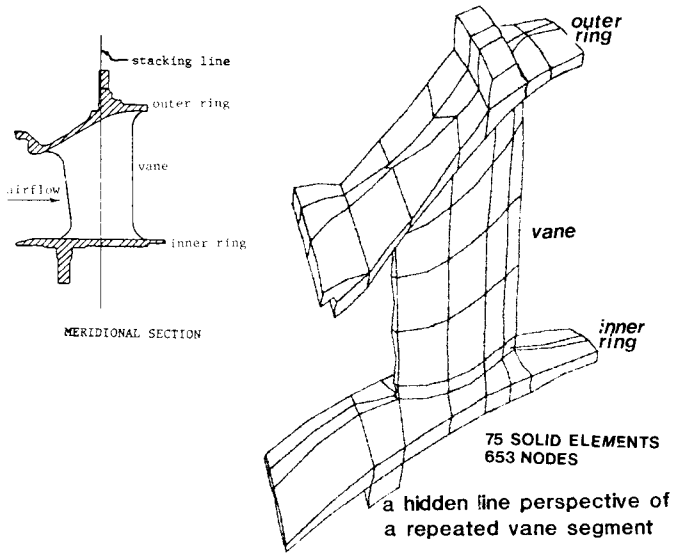

FIG. 8 F.E. MODEL OF TURBINE VANE RING

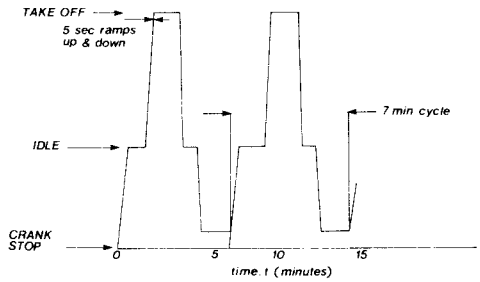

FIG. 9 SHORT CYCLIC ENDURANCE MISSION USED IN BLOCK TEST

The type of mission which was used in this study was a short cyclic endurance type mission between cold, ground idle and take-off conditions (shown in figure 9). The vane was primarily subjected to transient thermal loads arising from hot gas flow and external loads due to a pressure difference across its baffle attachment. All of these loads are schematically shown in figure 7.

Non-linear finite element thermal and stress analyses were carried out on the component throughout its mission. The same 20-node isoparametric solid elements were used in both analyses. Instantaneous temperature distributions were evaluated for successive time intervals throughout the time history. Subsequently they were followed with the strain-stress calculation for each load increment. With progressive plastic deformation, each increment of stress and strain was computed by iterating for equilibrium and was accumulated over the mission. The incremental formulation readily gives a pure elastic response to unloading. The plastic behaviour was characterized by von Mises yield criterion and its associated flow and hardening rules.

The above facilitated the evaluation in the mission its maximum principal normal strain ranges and mean strains by the method earlier developed. Figures 10 and 11 show isocontour plots of the mission maximum principal normal strain ranges and corresponding mean

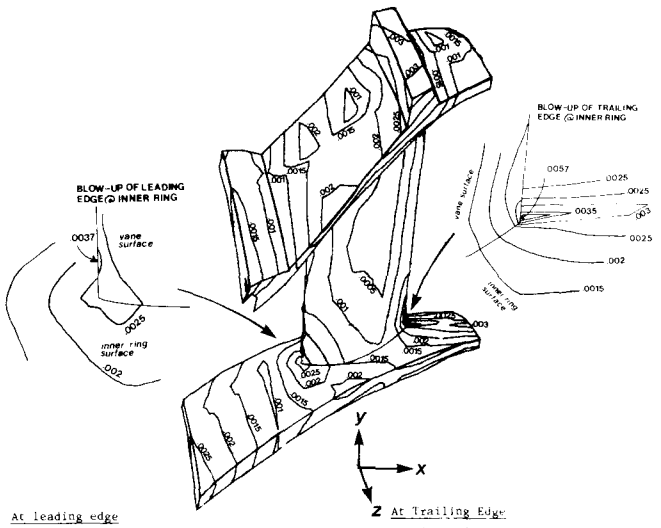

At leading edge

Mission principal normal strain range acting perpendicularly

θ_{xp}	θ_{yp}	θ_{zp}
74.	145.	120.

At Trailing Edge

Mission principal normal strain range acting perpendicularly

θ_{xp}	θ_{yp}	θ_{zp}
62.	34.	108.

FIG. 10 ISO-CONTOURS OF MISSION MAXIMUM PRINCIPAL NORMAL STRAIN RANGE ON VANE

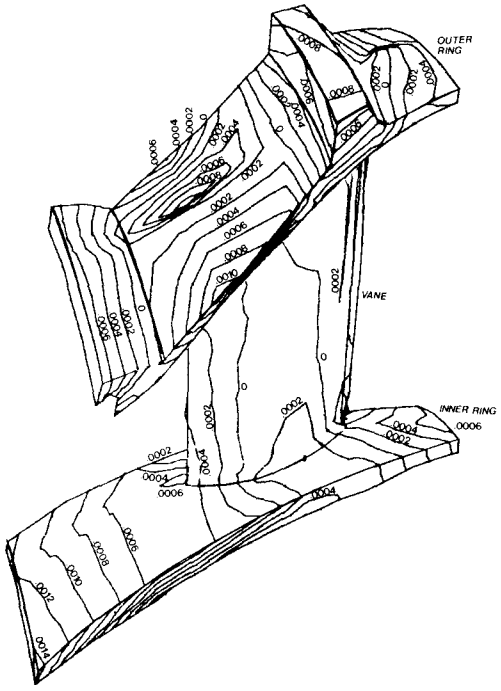

FIG. 11 ISO-CONTOURS OF NORMAL MEAN STRAINS ON VANE SURFACES

strains on the vanes' surface. Also shown in these figures are the directions at which the mission maximum principal normal strain range and mean strain act normal to. These are shown in a blown up view at the critical leading and trailing edge locations.

In order to analytically determine the low cycle fatigue life of the component what is needed in conjunction with the mission maximum principal normal strain range and mean strain is the fatigue behavior of the material, usually characterized by specimen testing. This is represented in terms of the total strain range versus the number of cycles to failure. In the case at hand the material used for the solid vane under study was INCO-792 a nickel based superalloy. During the mission, the vane was also subjected to thermal cycling in conjunction with primarily strain cycling. The baseline thermo-mechanical minimum(-3σ) fatigue life of this material is shown in figure 12 for temperature cycling limits between 426 and 982 °C and strain and temperature out of phase. Linking all of the above information allowed for a life prediction of the component. Figure 13 shows iso-contour plots of the life on the surface of the component.

As may be seen from this figure the most critical regions of this component seem to be concentrated at the airfoil junctions with the inner ring of the vane, on the leading and trailing edges. The predicted lives vary between 246 and 331 cycles at the leading edge root junction while they range between 38.5 and 316 cycles to failure at various locations at the trailing edge root junction.

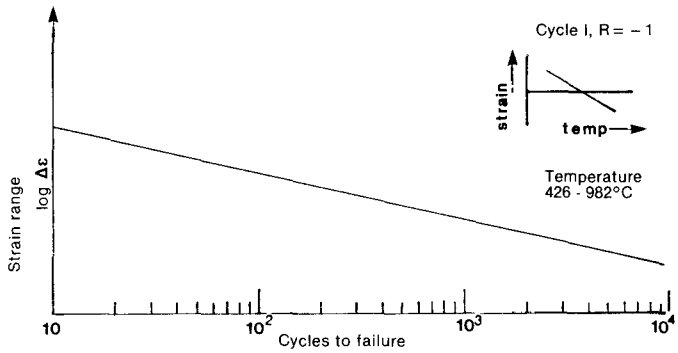

FIG. 12 MINIMUM (-3σ) BASELINE TMF PROPERTIES INCO-792

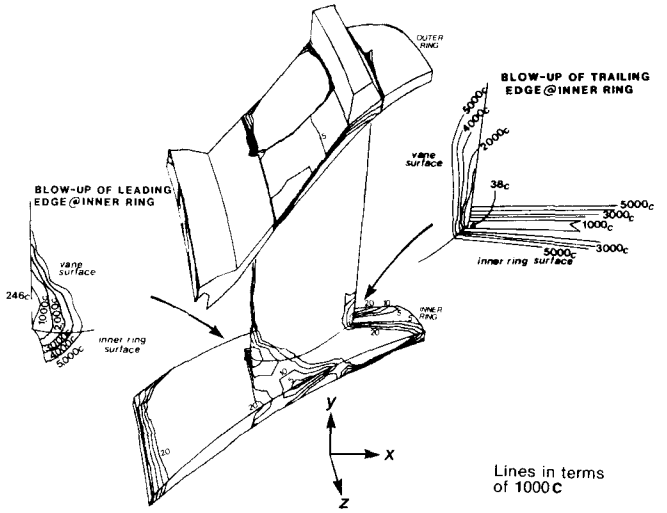

FIG. 13 ISO-LIFE LINES ON VANE SURFACES AND BLOW-UP OF CRITICAL REGIONS

Comparison to Test Rig Results

The results were compared to test rig results in order to evaluate the analytical life prediction. This involved one development turbine vane ring sustaining the type of cyclic loading depicted in figure 9. The

test rig was stripped down after 390 cycles of the type shown in figure 9. Subsequently microcracks were detected, at the vane leading and trailing edges, not visible to the naked eye(less than .80mm long). These cracks propagated at an angle of 45 degrees to the plane of the engine axis. The ratios of the predicted to actual lives range between 63% and 85% at the leading edge root junction and between 10% and 81% at the trailing edge root junction. The differences implies that an earlier rig strip would have shown cracks originating at the trailing edge. Figure 14 shows photographs of leading and trailing edge cracks on the vane after it had sustained 520 cycles of total running. Upon comparison of the orientation of these cracks (figure 14) with those predicted by analysis (figures 10 and 11) it may be seen that the two directly correspond.

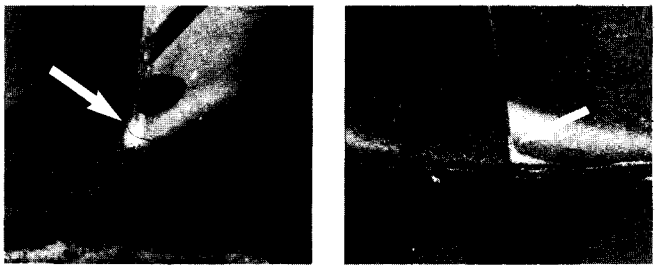

at leading edge at trailing edge

FIG. 14 CRACKS AT RING JUNCTURE ON ALL GUIDE VANES.

CONCLUSIONS

Design of turbine components subjected to high rotational speeds and temperatures is an ever-increasing area of interest in the gas turbine industry. This paper has examined the problem and has identified the need for very complex 3-D thermal, stress and life analysis to allow for more reliable gas turbine engine designs.

A method of determining the mission (cycle or subcycle) maximum principal normal strain range has been conceived and developed. The prerequisite for the use of this method is knowledge of the three dimensional state of strain, of the component, under mission loading. This state of strain may be determined from three dimensional finite element thermal and elasto-plastic stress analyses. The normal strain range function is then developed and its magnitude is maximized in time and three dimensional space. The space maximization reduces to an eigenvalue solution by the use of Lagrange multipliers while the time maximization is achieved by numerical scanning of all time step combinations in the mission.

In order to determine the creep behavior of a component a mission creep function was developed and maximized. This function may be established by prior knowledge of the components' creep behavior under each creep condition in the mission . This involves a three dimensional finite element creep rupture analysis for each creep condition in the mission. Once the behavior is established, a cumulative creep function is maximized with respect to space, by the use of Lagrange multipliers.

The life due to creep/fatigue interaction is evaluated by the ductility exhaustion method. It is determined in two principal directions; the direction of the mission (cycle or subcycle) maximum principal normal strain range and in the direction of maximum principal normal mission creep. The lowest life yielded by the above is considered in the integrity of the design.

The method has been applied to a solid (uncooled) vane and has been correlated to test rig experience. The results pertaining to life and crack orientation between analysis and rig testing are in excellent agreement.

In conclusion the approach presented has been successfully applied towards fatigue life prediction of available hardware. More effort should be devoted to calibrate and automate it. Furthermore the method should be implemented in and tested with more advanced non-linear damage accumulation concepts recently developed for creep/fatigue interaction.

REFERENCES

1 Timoshenko, S. and Goodier, J., "Theory of Elasticity", McGraw-Hill, New York, 2 nd Ed., 1951, pp 223.

2 Polhemus, J.F., Spaeth,C.E. and Vogel, W.H., "Ductility Exhaustion Model for Prediction of Thermal Fatigue and Creep Interaction", in: Thermal Fatigue at Elevated Temperatures, ASME STP 520, 1973, pp 625-635.

3 Ohji, K., Miller, W.R. and Marin, J., "Cumulative Damage and Effect of Mean Strain in Low-Cycle Fatigue of a 2024-T351 Aluminum Alloy", J. of Basic Engineering, Trans. ASME, Vol.88, Dec. 1966, pp 801-810.

4 Kaufman, A. and Gaugler, R., "Nonlinear, Three-dimensional Finite Element Analysis of Air-Cooled Gas Turbine Blades", NASA TP 1669, 1980.

5 Manson, S.S., Thermal Stress and Low Cycle Fatigue, Mc Graw-Hill 1966.

6 Manson, S.S. and Hirshberg, M.H., "Fatigue , An Interdisciplinary Approach", Syracuse University Press, Syracuse. N.Y., 1964, pp. 133-172.

7 Zamrik, S.Y. "The Application of SRP Method to Multiaxial Creep-Fatigue Interaction", Meeting on the SRP Method in Aalborg, Denmark, April 1978.

8 Halford, G.R., "High-Temperature Fatigue in Metals - A Brief Review of Life Prediction Methods Developed at the Lewis Research Center of NASA, SAMPE Quarterly, April 1983.

9 Sachs, G., Gerberich, W.W., Weiss, V. and Latorre, J.V., "Low-Cycle Fatigue of Pressure Vessel Materials", Proc. ASTM, vol. 60, 1960, pp 512-529.

10 Morrow, J.D. and Tuler, F.R., "Low Cycle Fatigue at Evaluation of Inconel 713 C and Waspaloy", J. of Basic Engineering, Trans. ASME, vol 60, 1961.

11 Zamrik, S.Y. and Frishmuth, R.E., "The Effects of Out of Phase, Biaxial Strain Cycling on Low Cycle Fatigue", SESA Fall Meeting 1969.

12 Mom, A.J., "Overview of the AGARD SMP Activities on Turbine Engine Materials Technology in the 1972-82 Period.

13 Lemaitre, J. and Chaboche, J.L., "Aspect phenomenologique de la rupture par endommagement", Journal de Mecanique Applique, vol 2, 1978, pp 317-365.

14 Gomuc, R. and Bui-Quoc, T., "Analysis of the Fatigue-Creep Behaviour of 304 Stainless Steel Using Continuous Damage Approach", 4 th Int. Conf. on Pressure Vessel & Piping, ASME San Antonio, Texas, June 1984.

15 Henderson, J., "An Investigation of Multi-axial Creep Characteristics of Metals", Transactions of the ASME, Vol 101, Oct 1979, pp 356-364.